Journal of Investigations on Engineering & Technology
Volume 8, Issue 1, 1-16, 2025
ISSN: 2687-3052

Research Article

Assessment of Soil Quality and Environmental Risk Using Multiple Pollution Indices: Avliyana (Gümüşhane, NE Türkiye)

Alaaddin VURAL[1]

(Received: 06.12.2026, Accepted: 26.12.2026, Published Online: 31.12.2025)

Assessment of Soil Quality and Environmental Risk Using Multiple Pollution Indices: Avliyana (Gümüşhane, NE Türkiye)

Keywords
Eastern Pontides
Soil pollution
Arsenic
Enrichment Factor
Environmental risk

Abstract: This study aims to determine the pollution levels and trace element enrichments of soils in the Avliyana area (Gümüşhane), located in the Eastern Pontide Orogenic Belt. The concentrations of Cr, Mn, Fe, Co, Ni, Cu, Zn, As, Cd, and Pb in the field soils were analyzed, and pollution levels were evaluated using the Pollution Index (PI), Geo-accumulation Index (Igeo), Enrichment Factor (EF), and Pollution Load Index (PLI). According to the findings, while Cr, Mn, Co, Ni, Cu, and Zn elements generally remained at natural background levels (EF < 2), distinct enrichments were detected in Arsenic (As), Cadmium (Cd), and Lead (Pb). Arsenic, in particular, was identified as the dominant pollutant in the area, with an average value of 82.74 ppm (maximum 533 ppm) and an Enrichment Factor (EF) exceeding 40. Comparison with local bedrock (granitoids and volcanics) data revealed that Arsenic is enriched approximately 42-fold in the soil compared to the parent rock, and this phenomenon is associated with anthropogenic effects and physicochemical processes (chemical trap) rather than a lithogenic origin. The Pollution Load Index (PLI) results indicate that environmental quality has deteriorated in the majority of the sampled points (13/16) and that certain locations exhibit "hotspot" characteristics.

1. Introduction

The Avliyana (Gümüşhane) area is situated within the Southern Zone of the Eastern Pontides Orogenic Belt, specifically at the transitional interface with the Northern Zone [1–8] (Figure 1). The study area falls within the administrative boundaries of Gümüşhane, a province with a mining heritage that traces back to antiquity [9, 10]. Historically referred to as *Argyropolis*—owing to its abundance of silver-bearing deposits alongside lead, zinc, and copper reserves—Gümüşhane has long been a significant center for mineral extraction [11, 12]. Contemporary geological assessments suggest that the region still harbors numerous undiscovered mineral deposits. Consequently, the area has been the subject of continuous exploration efforts, spanning from historical surveys to ongoing modern investigations [13–18] [3, 4, 24–30, 7, 10, 18–23] [24, 31–33] [11, 12, 16, 34–40].

[1] Author 1 Ankara University, Faculty of Engineering, Department of Geological Engineering, 06830 Gölbaşı, Ankara, Türkiye. *Orcid: 0000-0002-0446-828X*

Corresponding Author and e–mail address:

While mining activities are pivotal for national economic development, they have faced increasing social scrutiny, particularly following the latter half of the 20th century. The surge in environmental awareness, notably since the 1980s, has led to growing public opposition regarding such operations [41–44]. In recent years, the prevailing consensus has shifted towards approaches that equilibrate mining imperatives with environmental stewardship. By definition, a mining site represents a localized zone where specific elements are enriched beyond average crustal abundances. This implies a natural accumulation of elements, independent of anthropogenic inputs. Consequently, there exists an intrinsic relationship between elemental enrichment and potential toxicity within such geological settings [27, 45–49] [19, 23, 48, 50–54].

The primary objective of this study is to investigate the local enrichment thresholds and contamination risks within the Avliyana area, which is characterized by intense hydrothermal alteration and significant metallic enrichment, particularly in antimonite. To this end, the study focuses on determining the baseline concentrations of major trace elements in the soils of the region.

2. Regional geology

The study area is situated within the Eastern Pontides Tectonic Unit (EPTU), also referred to as the Pontide Tectonic Units [55]. Due to lithological distinctiveness observed between the northern and southern sectors during the Late Cretaceous, this region is traditionally examined under two separate headings: the Northern Zone and the Southern Zone [56],. However, Bektaş [57] and Bektaş and Güven [58] proposed a tripartite classification for the Eastern Pontides Magmatic Arc—dividing it from north to south into the Northern, Southern, and Axial Zones—based on variations in magmatism, tectonism, and sedimentological characteristics.

The basement of the EPTU is comprised of Early Carboniferous metamorphic rocks [59] and Early-Late Carboniferous plutonic intrusions [60–68]. These basement rocks are unconformably overlain by Early-Middle Jurassic volcano-sedimentary units [69, 70] and are intruded by Middle-Late Jurassic plutonic rocks [71]. The Late Jurassic-Early Cretaceous interval in the region represents a period of magmatic and tectonic quiescence, characterized by widespread carbonate deposition [72]. In contrast, the Late Cretaceous is represented by a diverse assemblage of plutonic, volcanic, and sedimentary rocks [5, 31, 73–78]. The Cenozoic stratigraphy of the region similarly consists of volcanic, plutonic, and sedimentary sequences [79, 80, 89–94, 81–88]. The youngest geological features in the region are slope debris, terraces, travertine, and alluvium [95–99].

The specific study area is located at the transition between the Northern and Southern Zones, though it predominantly exhibits Southern Zone characteristics. Lithologies ranging from the Paleozoic to the end of the Tertiary outcrop within the region [100–102]. The oldest stratigraphic units in the field are Permo-Carboniferous plutonic rocks, specifically the Artabel Granitoid [62, 103, 104]. These rocks are overlain by the Early-Middle Jurassic volcano-sedimentary Zimonköy Formation, separated by an erosional unconformity [100, 105, 106]. The Late Jurassic-Early Cretaceous Berdiga Formation conformably covers these underlying units [72].

Succeeding the Berdiga Formation is the Late Cretaceous Kermutdere Formation. This formation commences with sandy limestones at the base, transitions into purple limestones, and terminates with volcano-sedimentary units. It is also capped by Late Cretaceous andesites and basalts [5, 101, 107]. The Eocene Alibaba Formation—composed of andesites, basalts, and associated pyroclastics with intercalated sedimentary layers—rests unconformably upon the Kermutdere Formation. The entire stratigraphic sequence is intruded by the Lutetian-aged Avliyana Granitoid [2, 92, 101] (Figure 1). Finally, Quaternary alluvium, slope debris, and travertine represent the youngest formations in the area [104].

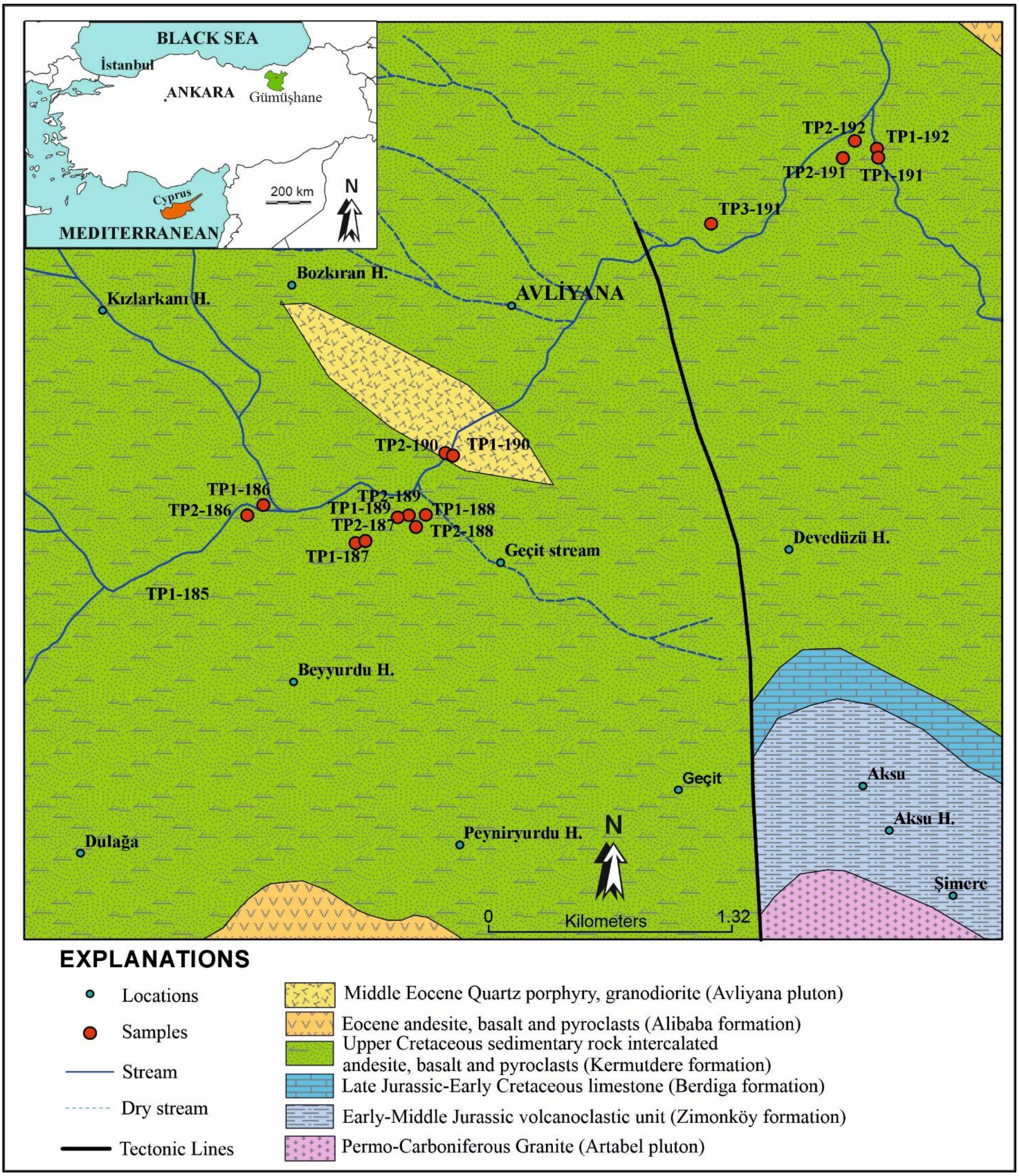

Figure 1. Geology of the study area and sampling locations[simplified from 2]

3. Materials and Methods: Soil Sampling, Analytical Procedures, and Pollution Indices

For the purpose of geochemical assessment, sixteen soil samples were collected from the upper soil profile (specifically the B horizon at depths of 10–25 cm) within the Avliyana area. To minimize potential contamination, a plastic spatula was employed for sample collection, and the materials were immediately stored in sterile plastic bags. Following initial air-drying at room temperature, the samples underwent oven-drying at 70–80 °C for two hours to eliminate residual moisture. The dried material was subsequently sieved to 2 mm, ground, and passed through an 80-mesh (~177 µm) screen, consistent with the optimal grain size recommendations of Rose et al. [45]. Selected trace element concentrations were determined using Inductively Coupled Plasma Atomic Emission Spectroscopy (ICP-AES) at the Gümüşhane University Central Laboratory. Prior to analysis, a microwave-assisted closed-system digestion procedure was utilized to obtain clear solutions. Specifically, 1 g aliquots of each soil

sample were initially treated with 2 ml of HNO_3 solution for one hour. Subsequently, 6 ml of a reagent mixture ($HCl–HNO_3–H_2O$ in a 2:2:2 ratio) was added. The solution was then digested at 95 °C for one hour before being introduced to the ICP-AES instrument. Comprehensive descriptions of the sample preparation and analytical protocols are provided in Vural [108, 109], Vural et al. [110], Vural and Erdoğan [111], and Bulut et al. [112].
To evaluate the extent of elemental enrichment—and by extension, potential contamination—the Geoaccumulation Index (Igeo), Pollution Index (PI), Enrichment Factor and Pollution Integrated Index were utilized. The Igeo classification, originally proposed by Müller [113], facilitates the assessment of pollution levels by comparing present-day metal concentrations against background (unenriched) values. This parameter is calculated using the following equation:

$$Igeo=log_2(Cn/1.5Bn) \quad (1)$$

In this equation, Cn represents the measured concentration of the element in the soil samples, while Bn denotes the geochemical background value, taken here as the average concentration of the corresponding element in the upper continental crust [114]. The constant factor of 1.5 was introduced by Stoffers et al. [115] as a matrix correction factor to account for potential lithogenic variations in the background data. For the interpretation of the Geoaccumulation Index, four distinct descriptive classes were adopted (Table 1).
Additionally, the Pollution Index (PI) is defined as the ratio of the specific element's concentration in the analyzed sample to its average abundance in the upper continental crust. To assess the level of elemental enrichment within the Avliyana area, PI values were computed and categorized according to the following criteria: no enrichment (PI<1.5) and enriched (PI ≥ 1.5).

Table 1. Classification of geoaccumulation index (Igeo) enrichment

Igeo Clas	Igeo value	Soil Quality / Pollution Level	Color in Table 5
0	Igeo≤0	Unpolluted	Blank
1	0<Igeo≤1	Unpolluted to moderately polluted	Yellow
2	1<Igeo≤2	Moderately polluted	Ivory
3	2<Igeo≤3	Moderately to strongly polluted	Blue
4	3<Igeo≤4	Strongly polluted	Pink
5	4<Igeo≤5	Strongly to extremely polluted	Khaki
6	Igeo>5	Extremely polluted	Red

4. Results

Descriptive statistics regarding the elemental composition of the Avliyana soil samples were calculated and are summarized in Table 2. Furthermore, the Pollution Index (PI) values for the studied soils were computed to illustrate the degree of enrichment (Table 3 and Figure 2), with the corresponding descriptive statistics provided in Table 4.

In Table 3, values ranging from 1.5 to 3 are highlighted in pink, representing PI levels that are noteworthy regarding potential pollution. Values exceeding 3.0 are marked in dark pink, corresponding to the "Extremely Polluted" category. The majority of the table remains uncolored, indicating that there is no significant contamination across the study area for most metals, particularly Cr, Ni, and Zn. However, based on the PI assessment, the area exhibits remarkable enrichment—and thus pollution—primarily in As, Cd, and Pb. Conversely, elements such as Cr, Mn, Ni, Cu, Zn, Co, and Fe show only sporadic or localized enrichment.

A closer examination of the data reveals that the PI_As column is particularly conspicuous. Notably, samples TP2-187 (PI=6.21) and TP1-187 (PI=6.03) exhibit the highest values, highlighted in bold dark pink.

Figure 2 illustrates the total pollution load for each sampling location based on the calculated PI data. This graph clearly identifies the specific sampling points subject to contamination. In the figure, the height of each bar represents the cumulative pollution load, while the color segments within the bars attribute the contamination to specific metals. Arsenic (depicted in grey/brown tones) constitutes the largest portion of the columns, confirming its status as the dominant pollutant in the region.

Table 2. Descriptive statistical parameters of the elements in the soils of the Avliyana site (ppm)

	Cr	Mn	Fe	Co	Ni	Cu	Zn	As	Cd	Pb
Mean	121.30	1313.80	6.48	25.15	72.10	54.39	98.88	82.74	0.27	37.38
Median	75.69	1085.25	5.91	23.13	56.68	49.35	85.91	23.30	0.21	26.39
Standart deviation	112.74	1025.68	3.71	12.45	42.44	42.68	42.98	164.61	0.18	23.02

Kurtosis	5.83	4.42	0.52	3.29	2.91	7.00	0.49	4.98	3.31	-0.28
Skewness	2.21	2.15	0.87	1.64	1.57	2.32	1.07	2.50	1.85	0.99
#	16.00	16.00	16.00	16.00	16.00	16.00	16.00	16.00	16.00	16.00
Maximum	471.20	4245.86	15.17	60.19	190.63	190.76	196.44	533.04	0.75	87.19
Minimum	19.30	381.28	1.96	11.00	24.80	12.68	50.90	6.61	0.10	9.79

Table 3. PI values of the elements in the soils of the Avliyana site. Values of 1.5 ≤ PI < 3 are shown in light pink, and PI ≥ 3 are shown in dark pink.

	PI_Cr	PI_ Mn	PI_Fe	PI_Co	PI_Ni	PI_Cu	PI_Zn	PI_As	PI_Cd	PI_Pb
TP1-187	5.12	5.48	1.66	3.48	4.06	1.91	2.63	**98.07**	3.62	3.41
TP1-189	2.52	4.22	1.95	2.33	2.35	1.94	2.93	12.80	3.80	3.80
TP1-191	2.01	1.50	1.36	1.46	2.35	2.08	1.52	5.02	2.22	1.75
TP2-186	1.62	1.66	2.48	1.60	1.57	2.56	1.33	2.83	2.50	1.26
TP2-187	0.78	0.49	3.88	1.35	1.86	6.81	1.58	**111.05**	1.12	1.17
TP2-188	0.65	2.23	3.10	1.53	1.13	1.99	1.74	4.12	2.82	3.50
TP2-189	0.70	1.21	2.12	1.14	0.89	1.33	0.98	5.85	2.03	1.41
TP2-190	1.48	1.21	2.15	1.32	0.91	1.02	0.90	1.38	1.24	0.58
TP2-191	2.16	1.40	1.28	1.44	2.43	1.61	1.24	9.10	2.22	1.39
TP2-192	0.53	1.57	1.87	0.83	1.03	0.59	2.08	6.01	8.34	5.13
TP3-191	0.30	0.84	0.68	0.74	0.53	2.57	1.89	1.56	3.33	1.98
TP1-185	0.87	0.65	0.55	0.86	0.97	0.45	0.83	1.92	2.33	1.25
TP1-186	0.87	1.03	0.96	2.24	1.51	3.28	0.93	4.69	2.22	1.69
TP1-188	0.58	0.78	0.79	1.05	1.29	1.11	0.76	3.94	1.11	1.37
TP1-190	0.71	1.40	1.17	1.25	0.98	1.31	1.09	2.02	1.78	1.21
TP1-192	0.21	1.46	0.50	0.64	0.69	0.50	1.18	5.46	6.67	4.27

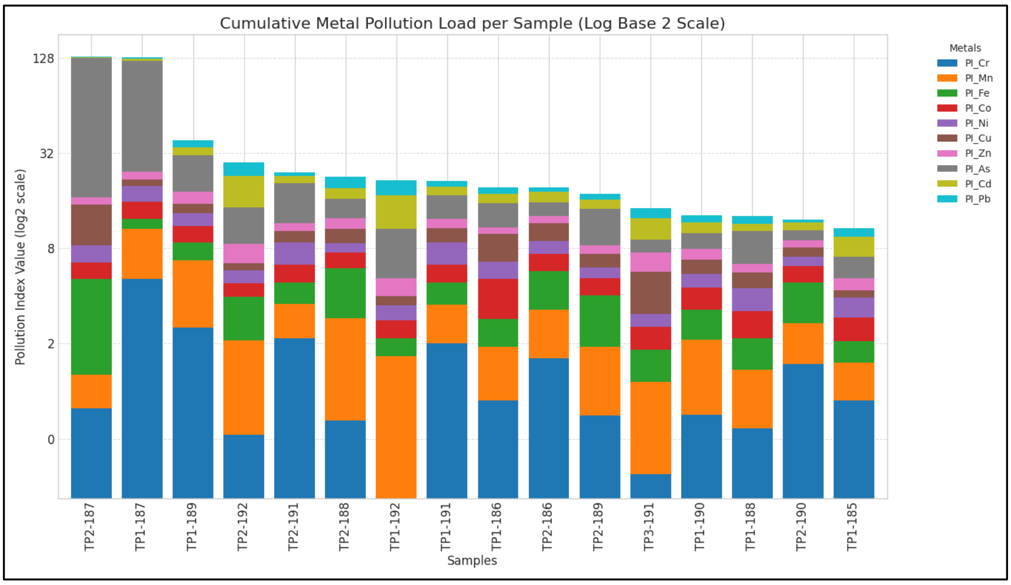

Figure 2. Cumulative total metal pollution load per sample in the Avliyana site

Table 4. Descriptive statistical parameters of the PI values of the elements in the soils of the Avliyana site

	PI_Cr	*PI_ Mn*	*PI_Fe*	*PI_Co*	*PI_Ni*	*PI_Cu*	*PI_Zn*	*PI_As*	*PI_Cd*	*PI_Pb*
Mean	1.32	1.70	1.66	1.45	1.53	1.94	1.48	17.24	2.96	2.20

Median	0.82	1.40	1.51	1.34	1.21	1.76	1.28	4.85	2.28	1.55
Standart deviation	1.23	1.32	0.95	0.72	0.90	1.52	0.64	34.29	1.97	1.35
Kurtosis	5.83	4.42	0.52	3.29	2.91	7.00	0.49	4.98	3.31	-0.28
Skewness	2.21	2.15	0.87	1.64	1.57	2.32	1.07	2.50	1.85	0.99
#	16.00	16.00	16.00	16.00	16.00	16.00	16.00	16.00	16.00	16.00
Maximum	5.12	5.48	3.88	3.48	4.06	6.81	2.93	111.05	8.34	5.13
Minimum	0.21	0.49	0.50	0.64	0.53	0.45	0.76	1.38	1.11	0.58

The calculated Igeo values for the study area are presented in Table 5, while the corresponding descriptive statistical parameters are provided in Table 6. Additionally, a box-and-whisker plot illustrating the Igeo distribution by element is depicted in Figure 4, which summarizes the general geochemical behavior and variability of each metal across the site. The dashed horizontal lines in the figure correspond to the Igeo classification thresholds (classes 0 to 5) defined by Müller [113].

According to the Igeo dataset, Arsenic (As) exhibits the widest distribution range and the highest mean values in the Avliyana area. The significant upward extension of the upper whisker for As indicates the presence of extremely high concentrations at specific sampling locations. Lead (Pb) and Cadmium (Cd) values predominantly fall within the 0–2 range ("Unpolluted to Moderately Polluted"). In contrast, for the remaining metals (Cr, Mn, Fe, Co, Ni, Zn), the majority of the box plots are positioned either below the zero line or slightly above it. This indicates that natural and/or anthropogenic accumulation for these elements is minimal, suggesting only partial or negligible enrichment.

Table 5. Igeo values of the soils from the Avliyana site

	Igeo_Cr	**Igeo Mn**	**Igeo_Fe**	**Igeo_Co**	**Igeo_Ni**	**Igeo_Cu**	**Igeo_Zn**	**Igeo_As**	**Igeo_Cd**	**Igeo_Pb**
TP1-187	1.77	1.87	0.15	1.21	1.44	0.35	0.81	6.03	1.27	1.19
TP1-189	0.75	1.49	0.38	0.64	0.65	0.37	0.97	3.09	1.34	1.34
TP1-191	0.42	0.00	-0.14	-0.04	0.65	0.47	0.02	1.74	0.57	0.22
TP2-186	0.11	0.15	0.72	0.10	0.07	0.77	-0.18	0.92	0.74	-0.25
TP2-187	-0.94	-1.61	1.37	-0.15	0.31	2.18	0.07	6.21	-0.42	-0.35
TP2-188	-1.22	0.57	1.05	0.03	-0.41	0.41	0.22	1.46	0.91	1.22
TP2-189	-1.10	-0.31	0.50	-0.39	-0.75	-0.17	-0.61	1.96	0.44	-0.08
TP2-190	-0.02	-0.31	0.52	-0.19	-0.73	-0.55	-0.73	-0.12	-0.27	-1.38
TP2-191	0.52	-0.10	-0.23	-0.06	0.69	0.11	-0.28	2.60	0.57	-0.11
TP2-192	-1.49	0.07	0.32	-0.85	-0.54	-1.35	0.47	2.00	2.47	1.77
TP3-191	-2.32	-0.84	-1.15	-1.02	-1.51	0.78	0.34	0.06	1.15	0.40
TP1-185	-0.79	-1.20	-1.43	-0.80	-0.63	-1.73	-0.85	0.35	0.64	-0.26
TP1-186	-0.79	-0.55	-0.65	0.58	0.01	1.13	-0.69	1.64	0.57	0.17
TP1-188	-1.36	-0.94	-0.93	-0.52	-0.22	-0.43	-0.98	1.39	-0.43	-0.13
TP1-190	-1.09	-0.10	-0.36	-0.26	-0.61	-0.20	-0.46	0.43	0.25	-0.31
TP1-192	-2.84	-0.04	-1.58	-1.24	-1.12	-1.59	-0.35	1.86	2.15	1.51

Table 6. Descriptive statistics of the Igeo values for the Avliyana site

	IgeoCr	***Igeo Mn***	***IgeoFe***	***IgeoCo***	***IgeoNi***	***IgeoCu***	***IgeoZn***	***IgeoAs***	***IgeoCd***	***Igeo_Pb***
Mean	-0.65	-0.11	-0.09	-0.19	-0.17	0.03	-0.14	1.98	0.75	0.31
Median	-0.87	-0.10	0.00	-0.17	-0.32	0.23	-0.23	1.69	0.60	0.04
Standart deviation	1.18	0.89	0.88	0.64	0.77	1.03	0.59	1.84	0.82	0.86
Kurtosis	0.05	0.90	-0.83	0.25	-0.20	0.24	-0.73	1.80	0.30	-0.47
Skewness	0.18	0.71	-0.22	0.42	0.35	-0.03	0.42	1.43	0.54	0.17
#	16.00	16.00	16.00	16.00	16.00	16.00	16.00	16.00	16.00	16.00
Maximum	1.77	1.87	1.37	1.21	1.44	2.18	0.97	6.21	2.47	1.77
Minimum	-2.84	-1.61	-1.58	-1.24	-1.51	-1.73	-0.98	-0.12	-0.43	-1.38

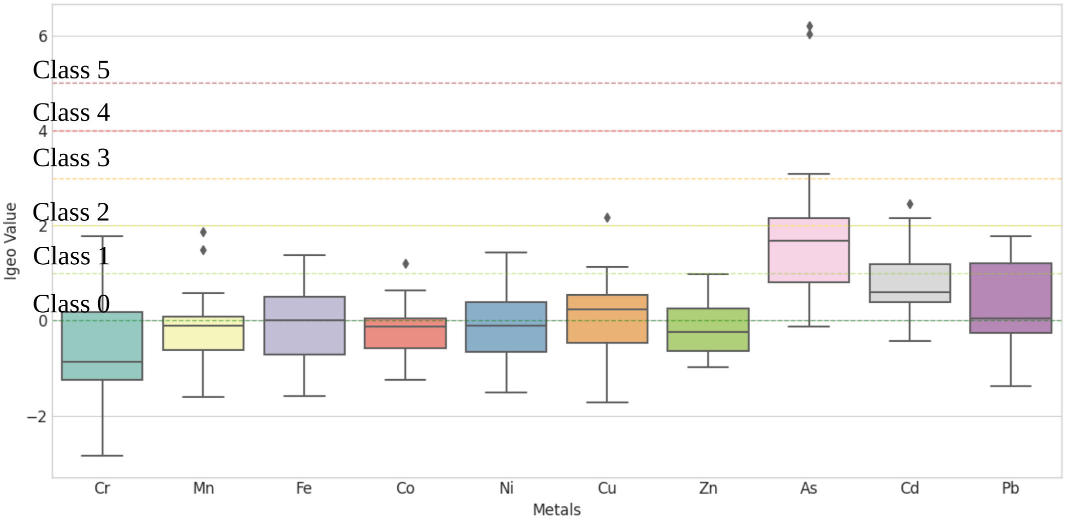

Figure 3. Box plot of the Igeo data for the study area

The Enrichment Factor (EF) was utilized to distinguish between lithogenic and anthropogenic sources of contamination within the study area (Figure 4). Iron (Fe) was selected as the reference element (normalizer) for these calculations, given its high natural abundance in the lithosphere and its relative immobility throughout geochemical processes.

Since the Pollution Index (PI) dataset was already available, Enrichment Factor (EF) values for each element were calculated using the relationship **EF = PI_element / PI_Fe.** Because PI values are normalized to upper continental crust abundances, deriving EF values from PI ratios ensures internal consistency among the applied pollution indices. Based on the classification scheme proposed by Sutherland [116], an EF box-and-whisker plot was generated (Figure 5). The elements Cr, Mn, Co, Ni, Cu, and Zn predominantly fall within the range of EF < 2 ("Deficiency to Minimal Enrichment"), suggesting that their presence is primarily governed by the parent rock lithology (natural geological background). In contrast, Cadmium (Cd) and Lead (Pb) exhibited slight elevations in certain samples, corresponding to "Moderate Enrichment" (EF 2–5). Arsenic (As) emerges as the most conspicuous element in the graph, with values exceeding 40 ("Extremely High Enrichment"). The high EF values identified in the field sampling records provide strong evidence that the contamination at these locations is of anthropogenic origin, most likely associated with sources such as mining residues (tailings) and/or agricultural pesticides.

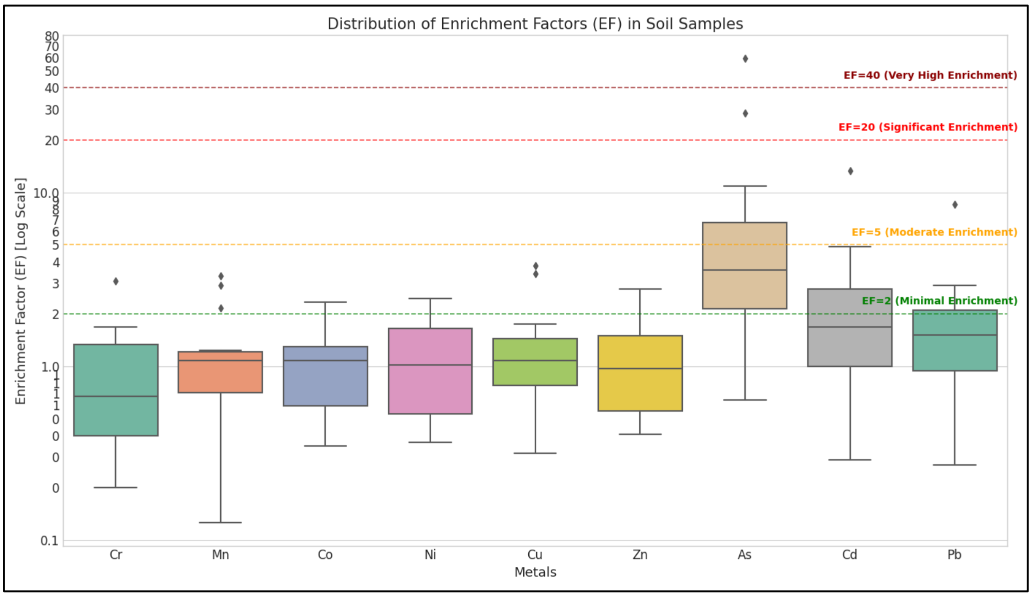

Figure 5. Box plot of the EF data for the site

Within the scope of the environmental geochemical investigation conducted on the Avliyana site soils, the Pollution Load Index (PLI) was additionally utilized to extend the interpretation beyond individual metal concentrations and to obtain an integrated measure of the area's overall heavy-metal contamination. Introduced by Tomlinson [117], the PLI represents a key indicator that condenses the collective impact of multiple contaminants into **one composite value**, thereby reflecting the general pollution intensity of the site.

The index serves several important functions:

- Quantifying Overall Contamination Pressure: It integrates the concentrations of various heavy metals to express their combined environmental burden.
- Enabling Comparative Assessments: It allows objective comparison of the pollution status of the study area either through time or in relation to other locations.

Interpretation of PLI values follows a simple framework:

- **PLI ≤ 1** denotes an absence of contamination.
- **PLI > 1** indicates the presence of pollution, with increasing values corresponding to greater levels of environmental degradation.

PLI is calculatede as follow:

$$PLI = \sqrt[n]{PI_1 x PI_2 x PI_3 \ldots . x PI_n} \qquad 2$$

where n**:** The number of metals analyzed.

The PLI results indicate that the majority of the samples (13 out of 16) exhibit PLI values greater than 1, demonstrating a general decline in environmental quality and the presence of a measurable metal pollution load across the study area. The highest levels of contamination were recorded in samples TP1-187 (PLI = 4.87) and TP1-189 (PLI = 3.25), which can be classified as contamination "hotspots," largely driven by elevated arsenic (As) concentrations. In contrast, only three samples—TP3-191 (PLI = 0.97), TP1-185 (PLI = 0.91), and TP1-192 (PLI = 0.91)—display PLI values below 1. These locations may therefore be considered unpolluted or representative of natural background conditions (Figure 6).

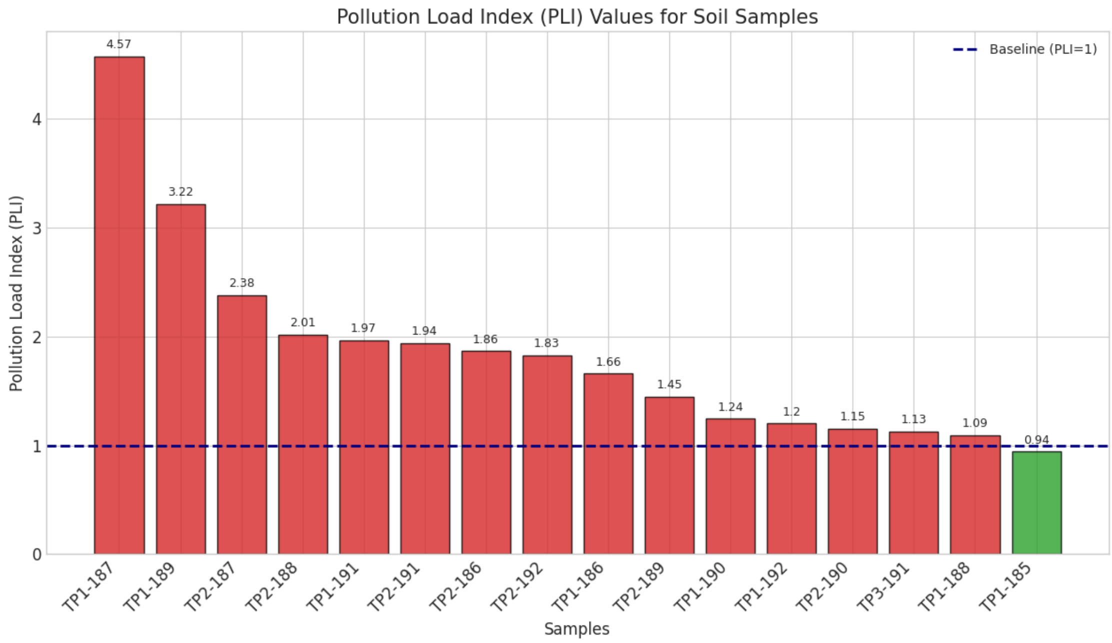

Figure 6. Bar chart of the Pollution Load Index for the Avliyana site

5. Discussion

In order to more clearly elucidate the geochemical cycling within the study area, the soil data obtained in this investigation were compared with the average values of bedrock analyses (granitoids and volcanics) previously reported by Vural and Kaygusuz [107] from the same locality. Using these datasets, a Rock–Soil Elemental Enrichment Diagram was constructed for the site (Figure 7).

Examination of Figure 7 reveals that Cu and Zn display relatively moderate enrichment in soils compared to the bedrock, with enrichment factors ranging from approximately 1.1 to 3.3. This pattern is consistent with the capacity of clay minerals to adsorb these metals during pedogenic processes. In contrast, the behavior of arsenic (As) is markedly different; while the average As concentration in bedrock is around ~2 ppm [107], the soils exhibit a mean concentration of 82.7 ppm.

The calculated enrichment coefficients (Soil/Rock ratios) further show that arsenic is enriched by approximately 42-fold relative to its bedrock levels (Figure 7). Such an extreme increase cannot be explained solely by the physical disintegration of the parent rock. Instead, it suggests that arsenic mobilized through a combination of hydrothermal inheritance, surface weathering, and subsequent remobilization under anthropogenic influences (e.g., agricultural practices), with a possible minor contribution from acid mine drainage (AMD) processes — previously described in Vural [4]—may have been retained within the soil profile by iron–manganese oxides and organic matter, acting as a “chemical trap” and leading to progressive accumulation over time. The retention of arsenic by Fe–Mn oxides and organic matter is a well-documented process in oxidizing soil environments and plays a key role in long-term arsenic accumulation.

In summary, while the bedrock geochemistry indicates the potential source of contamination, the soil data and associated enrichment patterns presented in this study demonstrate how this potential has manifested as an actual environmental risk under surface conditions.

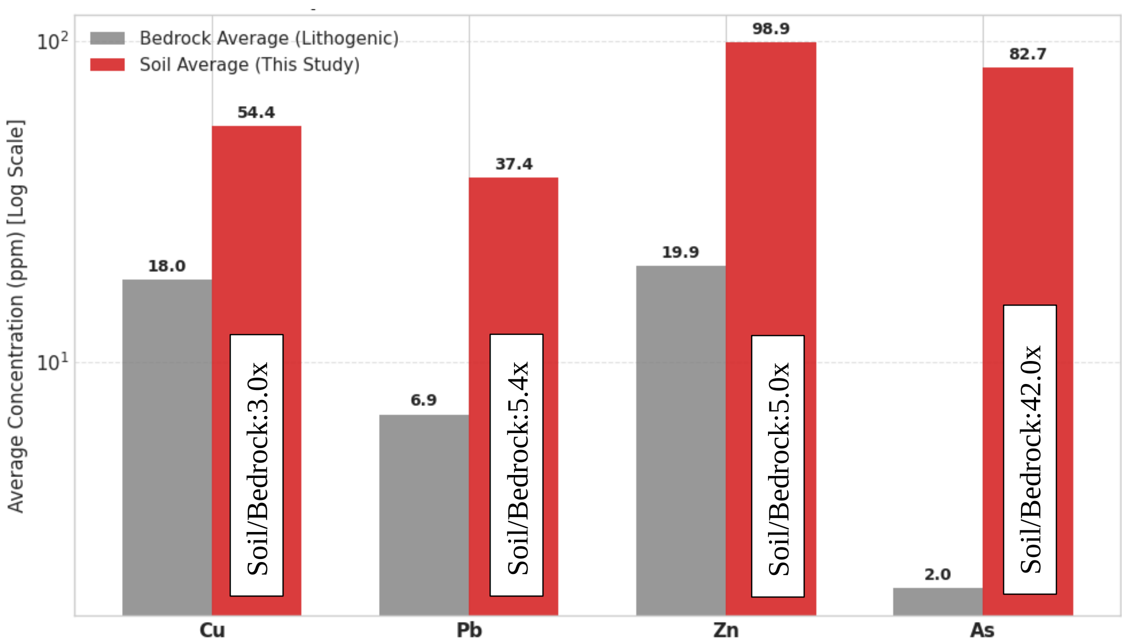

Figure 7. Element concentrations in bedrock and soil, and elemental enrichment of soils relative to bedrock

A comparison was made between the data obtained in this study and the results reported by Vural and Çiçek (2022) for soils developed over the stibnite mineralization, which partially overlaps with the present study area. This comparison was visualized using a bar diagram (Figure 8).

As shown in Figure 8, when the element concentrations of soils overlying the mineralization zone are evaluated together with the concentrations measured at the sampling locations of this study, a striking difference is observed in arsenic (As) levels. While the average As content in soils overlying the mineralization was reported as 10.98 ppm (maximum: 20.50 ppm), the Avliyana soils investigated here display a mean As concentration of 82.74 ppm (maximum: 533 ppm), indicating an enrichment approximately 7.5 times higher.

This pronounced increase is interpreted as evidence of anthropogenic influence associated with agricultural activities at the sampling locations of the present study. Although the samples collected by Vural and Çiçek [7] were taken from areas situated above the mineralization zone, the absence of direct contact with the ore body was highlighted as the likely reason for the lower arsenic levels they reported.

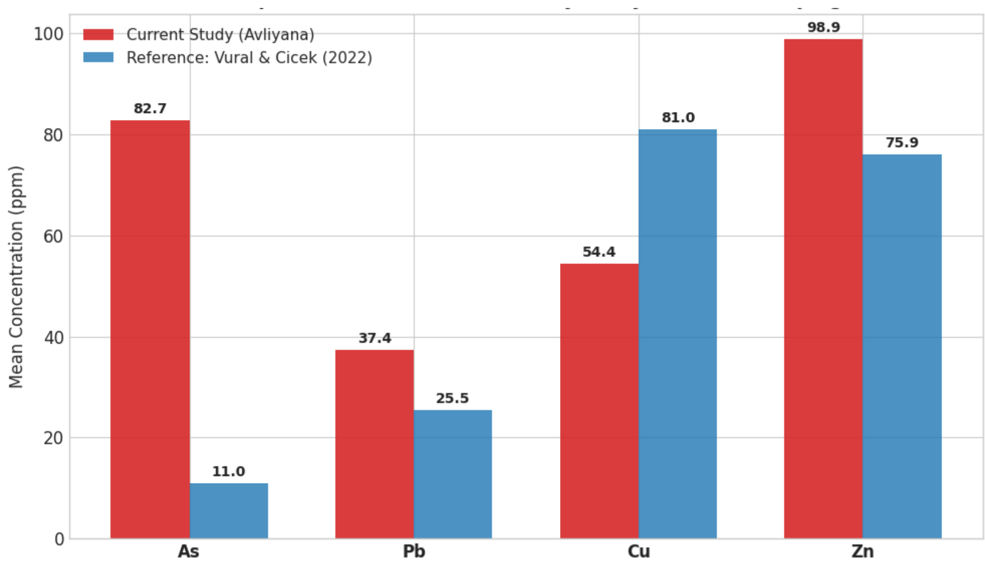

Figure 8. Bar chart comparing As, Pb, Cu, and Zn concentrations in soils overlying the stibnite mineralization and in the study area soils

6. Conclusions

The findings obtained from this study, conducted to determine the geochemical characteristics of the soils in the Avliyana (Torul) area of Gümüşhane Province (Northeastern Türkiye), assess elemental enrichment levels, and evaluate the associated environmental risks, are summarized below:

• **Elemental Distribution and Dominant Contaminants:** The spatial distribution of elements in the study area soils is not homogeneous. While Cr, Mn, Co, Ni, Cu, and Zn generally occur at low concentrations within natural background ranges, pronounced anomalies were detected for arsenic (As), lead (Pb), and cadmium (Cd). Among these, arsenic stands out as the most dominant contaminant, with an average concentration of 82.74 ppm and a maximum of 533 ppm.

• **Pollution Indices and Anthropogenic Influence:** Evaluations based on the Geoaccumulation Index (Igeo) and Enrichment Factor (EF) provide critical insights into the origin of elemental inputs. EF values below 2 for elements such as Cr, Mn, Ni, and Zn indicate predominantly lithogenic (bedrock-derived) sources. In contrast, arsenic exhibits EF values exceeding 40 in nearly all samples—classified as "Extremely High Enrichment"—and appears in the "Extremely Polluted" category according to the Igeo scale. These results indicate that arsenic accumulation is influenced not only by natural geological processes but also by hydrothermal/mineralization-related contributions, agronomic inputs, and secondary anthropogenic impacts derived from the transport of materials associated with mineralized zones.

• **Bedrock–Soil Relationship:** Comparison of the soil data with the geochemical composition of granitoid and volcanic bedrock units from the same region [107] further clarifies the magnitude of contamination. Elements such as Cu and Zn show moderate enrichment during soil formation, ranging from 1.1 to 3.3 times their bedrock concentrations. However, arsenic displays striking enrichment—approximately 42-fold relative to bedrock levels. This extreme increase suggests that arsenic mobilized through processes such as Acid Mine Drainage (AMD) may have been retained within the soil by iron–manganese oxides and organic matter, operating as a "chemical trap" that promotes long-term surface accumulation.

• **Regional Comparison and Agricultural Pressure:** When compared to soils developed above stibnite mineralization in the same region [7], the Avliyana soils exhibit arsenic concentrations approximately 7.5 times higher. The elevated As levels observed at locations without direct contact with the mineralized zone likely reflect additional contamination arising from regional agricultural practices or the redistribution of legacy mining materials.

• **Overall Environmental Risk:** According to the Pollution Load Index (PLI), more than 81% of the sampled locations (13 out of 16) display PLI values greater than 1, indicating a widespread contamination pressure affecting soil quality across the area. Locations such as TP1-187 and TP1-189 represent contamination "hotspots" with exceptionally high metal burdens, highlighting the need for focused environmental monitoring and potential remediation.

In conclusion, the soils of the Avliyana area are subject to a notable contamination pressure that exceeds the natural geochemical signature of the underlying bedrock, particularly with respect to arsenic. This contamination poses a potential risk to both regional ecosystem integrity and agricultural production safety.

Acknowledgements

This study partially utilizes data generated within the scope of the TÜBİTAK-funded Project No. 115Y146. The authors gratefully acknowledge TÜBİTAK for its financial support. The authors also wish to thank the editor for their valuable contributions during the publication process, as well as the anonymous reviewers for their constructive comments and suggestions, which significantly contributed to the improvement of the manuscript.

Author Contribution

The author solely conceived and designed the research, conducted all fieldwork and sampling, performed the laboratory analyses, processed and interpreted the geochemical data, prepared the figures and tables, and wrote and revised the manuscript in its entirety. All stages of the study, from conceptualization to final editing, were carried out exclusively by the author.

Conflict of Interest

The author confirms that there is no known conflict of interest or common interest with any institution/organization or person.

References

[1] Sungur, A., Vural, A., Gundogdu, A., Soylak, M., Effect of antimonite mineralization area on heavy metal contents and geochemical fractions of agricultural soils in Gümüşhane Province, Turkey. *Catena* 2020, *184*.

[2] Vural, A., K-Ar dating for determining the age of mineralization as alteration product: A case study of antimony mineralization vein type in granitic rocks of Gümüşhane area, Turkey. *Acta Phys. Pol. A* 2017, *132*, 792–795.

[3] Vural, A., Gündoğdu, A., Saka, F., Bulut, V.N., Geochemical investigation of the potability of surface water in Çit Stream and related creeks in Avliyana Basin (Gümüşhane , NE Türkiye). *Turkish J. Anal. Chem.* 2022, *4*, 44–51.

[4] Vural, A., Avliyana Cevherleşme/Alterasyon Sahasının Kütle Değişim Özellikleri ve Asit Maden Drenaj Potansiyelinin Araştırılması. *Icontech Int. J. Surv. Eng. Technol.* 2022, *6*, 1–23.

[5] Vural, A., Kaygusuz, A., Petrographic and geochemical characteristics of late Cretaceous volcanic rocks in the vicinity of Avliyana (Gümüşhane, NE Turkey). *J. Eng. Res. Appl. Sci.* 2021, *10*, 1796–1810.

[6] Sungur, A., Vural, A., Gündoğdu, A., Soylak, M., Gümüştuğ Köyü (Torul-Gümüşhane) Tarım Topraklarında Manganın Jeokimyasal Karakterizasyonu, in: *International Trace Analysis Congress (ITAC 2018/ES-AN 2018)*, Sivas, Türkiye 2018, p. 231.

[7] Vural, A., Çicek, B., Evaluation of Gümüştuğ Antimonite (Torul , Gümüşhane/Türkiye) Mineralization with Soil Geochemistry and Multivariate Geostatistical Studies. *J. Eng. Res. Appl. Sci.* 2022, *11*, 2156–2170.

[8] Vural, A., Çiçek, B., Gümüştuğ Antimonit Cevherleşmesinin Toprak Jeokimyası ve Titrek Kavak (Populus Tremula)'nın Biyojeokimyasal Özelliklerinden Yararlanılarak Araştırılması, Gümüşhane, Türkiye 2021.

[9] Vural, A., Kaya, S., Başaran, N., Songören, O.T., Anadolu Madenciliğinde İlk Adımlar, Maden Tetkik ve Arama Genel Müdürlüğü, MTA Kültür Serisi-3, Ankara, Türkiye 2009.

[10] Vural, A., Erşen, F., Geology, mineralogy and geochemistry of manganese mineralization in Gumushane, Turkey. *J. Eng. Res. Appl. Sci.* 2019, *8*, 1051–1059.

[11] Vural, A., Corumluoglu, Ö., Asri, İ., Remote sensing technique for capturing and exploration of mineral

deposit sites in Gumushane metallogenic province, NE Turkey. *J. Geol. Soc. India* 2017, *90*, 628–633.

[12] Vural, A., Çorumluoğlu, Ö., Asri, İ., Investigation of alteration areas by Crosta using LANDSAT images for Old Gumushane (Suleymaniye) and its near vicinity. *J. Nat. Sci. Inst. Gumushane Univ.* 2012, *2*, 36–48.

[13] Özdoğan, K., Karadağ (Torul-Gümüşhane) ve Yakın Çevresinin Jeolojisi-Mineralojisi-Petrografisi ve Maden Zuhurlarının Jenetik İncelenmesi, Selçuk Üniversitesi, 1992.

[14] Lermi, A., Midi (Karamustafa/Gümüşhane, KD Türkiye) Zn-Pb Yatağının Jeolojik, Mineralojik, Jeokimyasal ve Kökensel İncelemesi, K.T.Ü. Trabzon, Türkiye, 2003.

[15] Demir, Y., Istala ve Köstere (Zigana/Gümüşhane) Cu-Pb-Zn Madenleri ve Yan Kayaçlarının Mineralojisi ve Dokusal Özelliklerinin Karşılaştırılmalı İncelenmesi, K.T.Ü. Trabzon-Türkiye, 2005.

[16] Vural, A., Gold and Silver Content of Plant Helichrysum Arenarium, Popularly Known as the Golden Flower, Growing in Gümüşhane, NE Turkey. *Acta Phys. Pol. A* 2017, *132*, 978–980.

[17] Vural, A., Gündoğdu, A., Saka, F., Bulut, V.N., et al., The Heavy Metals and Minor Elements Effects of Mineralization and Alteration Areas with Buried Ore Deposits Potential on the Surface Waters. *J. Investig. Eng. Technol.* 2022, *5*, 21–33.

[18] Vural, A., Evaluation of soil geochemistry data of Canca Area (Gümüşhane, Turkey) by means of Inverse Distance Weighting (IDW) and Kriging methods-preliminary findings. *Bull. Miner. Res. Explor.* 2019, *158*, 195–216.

[19] Vural, A., Kaygusuz, A., The Geostatistical Evaluation of the Genetic Relationship of Rocks : A Case Study of the Derinoba-Kayadibi Granites. *J. Eng. Res. Appl. Sci.* 2024, *13*, 2537–2552.

[20] Vural, A., On the elemental contents of aspen (Populus tremula L.) leaves grown in the mineralization area. *J. Geogr. Cartogr.* 2023, *6*, 1–10.

[21] Vural, A., Safari, S., Phytoremediation ability of Helichrysum arenarium plant for Au and Ag: case study at Demirören village (Gümüşhane, Turkey). *Gold Bull.* 2022, *55*, 129–136.

[22] Vural, A., Akpinar, İ., Sipahi, F., Mineralogical and Chemical Characteristics of Clay Areas, Gümüşhane Region (NE Turkey), and Their Detection Using the Crósta Technique with Landsat 7 and 8 Images. *Nat. Resour. Res.* 2021, *30*, 3955–3985.

[23] Vural, A., Biogeochemical characteristics of Rosa canina grown in hydrothermally contaminated soils of the Gümüşhane Province, Northeast Turkey. *Environ. Monit. Assess.* 2015, *187*, 486.

[24] Vural, A., Demirören/Gümüşhane-Türkiye Kuvars Porfiri Kayacı ve İlişkili Skarn-Metasomatizmanın Jeokimyasal Özellikleri. *Euroasia J. Math. Eng. Nat. Med. Sci.* 2020, *7*, 97–121.

[25] Özkan, M., Vural, A., Akgül, Ö., Gültepe, M.A., et al., Comprehensive geostatistical Assessment of stream sediments for mineralization potential in the eastern Black Sea region. *Period. Di Mineral.* 2025, *94*, 83–111.

[26] Vural, A., Kaya, A., Arzular-Yitirmez-Dölek (Gümüşhane) Maden/Alterasyon Sahalarındaki Doğal (226Ra, 232Th ve 40K) ve yapay (138Cs) Radyoaktivitelerine ait ilk değerlendirmeler. *Euroasia J. Math. Eng. Nat. Med. Sci.* 2021, *8*, 105–120.

[27] Vural, A., Trace element accumulation behavior, ability, and propensity of Taraxacum officinale F.H. Wigg (Dandelion). *Environ. Sci. Pollut. Res.* 2024, *31*, 16667–16684.

[28] Vural, A., Kaya, A., Assessment of Karamustafa Gold-Bearing Zn-Pb Mine (Gümüşhane, Türkiye) Area in Terms of Natural and Artificial Radioactivity. *Göbeklitepe Int. J. Med. Sci.* 2023, *6*, 39–52.

[29] Vural, A., Trace/heavy metal accumulation in soil and in the shoots of acacia tree, Gümüşhane-Turkey. *Bull. Miner. Res. Explor.* 2014, *148*, 85–106.

[30] Hou, Z., Zhang, H., Geodynamics and metallogeny of the eastern Tethyan metallogenic domain. *Ore Geol. Rev.* 2015, *70*, 346–384.

[31] Sipahi, F., Saydam Eker, Ç., Akpınar, İ., Gücer, M.A., et al., Eocene magmatism and associated Fe-Cu mineralization in northeastern Turkey: a case study of the Karadağ skarn. *Int. Geol. Rev.* 2022, *64*, 1530–1555.

[32] Sipahi, F., Kaygusuz, A., Saydam Eker, Ç., Vural, A., et al., Late Cretaceous arc igneous activity: the Eğrikar Monzogranite example. *Int. Geol. Rev.* 2018, *60*, 382–400.

[33] Sipahi, F., Akpınar, İ., Gücer, M.A., Kaygusuz, A., et al., Origin and tectonic setting of the carbonate-hosted Kopuz Fe skarn Deposit, Sakarya Zone, NE Türkiye. *J. Asian Earth Sci.* 2025, *294*, 106769.

[34] Akçay, M., Lermi, A., Van, A., Biogeochemical exploration for massive sulphide deposits in areas of dense vegetation: An orientation survey around the Kankoy Deposit. *J. Geochemical Explor.* 1998, *63*, 173–187.

[35] Lermi, A., Midi (Karamustafa/Gümüşhane, KD Türkiye) Zn-Pb Yatağının Jeolojik, Mineralojik, Jeokimyasal ve Kökensel İncelemesi, Karadeniz Teknik Üniversitesi, Trabzon, 2003.

[36] Sipahi, F., Akpınar, İ., Saydam Eker, Ç., Kaygusuz, A., et al., Formation of the Eğrikar (Gümüşhane) Fe–Cu skarn type mineralization in NE Turkey: U–Pb zircon age, lithogeochemistry, mineral chemistry, fluid inclusion, and O-H-C-S isotopic compositions. *J. Geochemical Explor.* 2017, *182*, 32–52.

[37] Vural, A., Assessment of Sessile Oak (Quercus petraea L.) Leaf as Bioindicator for Exploration Geochemistry. *Acta Phys. Pol. A* 2016, *130*, 191–193.

[38] Sipahi, F., Saydam Eker, Ç., Akpınar, İ., Gücer, M.A., et al., Eocene magmatism and associated Fe-Cu mineralization in northeastern Turkey: a case study of the Karadağ skarn. *Int. Geol. Rev.* 2021, 1–26.

[39] Sipahi, F., Saydam Eker, Ç., Kaygusuz, A., Vural, A., Investigation of mineral chemistry, fluid inclusion and stable isotope composition of skarn mineralization at Eğrikar (Torul-Gümüşhane, NE Turkey), Ankara, Turkey 2016.

[40] Ünal Çakır, E., Gökce, A., Geology, fluid inclusion, and stable isotope (O, H, S, C) characteristics of the Hazinemağara (Gümüşhane) lead-zinc deposit , NE Turkey. *Turkish J. Earth Sci.* 2019, *28*, 623–639.

[41] Çiftçi, A., Ural, M.N., Vural, A., Baz metallerin dünya siyasi tarihindeki önemli olaylarla bağlantısının retrospektif literatür taramasi yöntemi ile araştırılması. *Int. Soc. Sci. Stud. J.* 2020, *6*, 1453–1461.

[42] Çiftçi, A., Vural, A., Ural, M.N., Analysis of Some Concepts Related to the Environment and Health with the N-Gram Method. *J. Int. Heal. Sci. Manag.* 2021, *7*, 47–54.

[43] Bilimsel, M.T., Analysis, R., Example, T., Fak, B., et al., Mağaralarda Jeoturizm Amaçlı Risk Analizi; Gümüşhane Akçakale Mağarası Örneği. 2025, 35–45.

[44] Külekçi, G., Exploration of Chemical Composition and Properties of Ancient Silver Mine Slag. *J. Civ. Eng. Constr.* 2025, *14*, 1–7.

[45] Rose, A.W., Hawkes, H., Webs, J., Geochemistry in Mineral Exploration, 2nd ed., Academic Press, Londan, England 1991.

[46] Reis, A.P., Sousa, A.J., Cardoso Fonseca, E., Soil geochemical prospecting for gold at Marrancos (Northern Portugual). *J. Geochemical Explor.* 2001, *73*, 1–10.

[47] Vural, A., Investigation of the relationship between rare earth elements, trace elements, and major oxides in soil geochemistry. *Environ. Monit. Assess.* 2020, *192*, 124.

[48] Vural, A., Soil geochemistry survey for gold exploration at Kısacık area (Çanakkale, Ayvacık, Türkiye). *Period. Di Mineral.* 2024, *93*, 61–83.

[49] Vural, A., Comparison of Threshold Values Calculated with Different Methods and Soil Geochemistry Survey Using Iso-concentration Mapping for Single Element and Multielement Halos Technique for Gold Exploration at Kısacık (Ayvacık/Çanakkale-Türkiye). 2023, (under review).

[50] Reimann, C., Garrett, R.G., Geochemical background - Concept and reality. *Sci. Total Environ.* 2005, *350*, 12–27.

[51] Ellsmore, R., Buckman, S., Soil geochemistry and pathfinder element distribution associated with the Hillgrove Antimony-Gold-Tungsten deposit, New England Orogen, NSW. *New Engl. Orogen 2010* 2010, *2010*, 141–144.

[52] Hao, L., Zhao, X., Zhao, Y., Lu, J., et al., Determination of the geochemical background and anomalies in areas with variable lithologies. *J. Geochemical Explor.* 2014, *139*, 177–182.

[53] Külekçi, G., Vural, A., Analysis and Classification of Water Occuring Naturally in a Metallic Underground Mine, in: *International Halich Congress*, İstanbul, Türkiye 2021, pp. 308–316.

[54] Saydam Eker, Ç., Külekçi, G., Uçak, G., First evaluation and ecological risk of potentially toxic elements in the formations of Akçakale cave (Gümüşhane-NE-Türkiye). *Environ. Monit. Assess.* 2025, *197*, 1–24.

[55] Ketin, İ., Canitez, N., Yapısal Jeoloji, İstanbul İTÜ Kütüphanesi 1972.

[56] Özsayar, T., Pelin, S., Gedikoğlu, A., Doğu Pontidlerde Kretase. *KTÜ Yer Bilim. Derg.* 1981, *1*, 65–114.

[57] Bektaş, O., Upper Cretaceous shoshonitic volcanism and its importance in the eastern Pontides. *Karadeniz*

Tech. Univ. Earth Sci. Bull. 1984, *3*, 53–62.

[58] Bektaş, O., Güven, İ.H., Alaskan Aphinitic Type Ultramafic and Mafic Complexes as the Root Zone of the Eastern Pontide Magmatic Arc (NE Turkey), in: *Geology of the Black Sea Region*, Ankara, Türkiye 1995, pp. 189–196.

[59] Topuz, G., Altherr, R., Kalt, A., Satir, M., et al., Aluminous granulites from the Pulur complex, NE Turkey: A case of partial melting, efficient melt extraction and crystallisation. *Lithos* 2004, *72*, 183–207.

[60] Topuz, G., Altherr, R., Siebel, W., Schwarz, W.H., et al., Carboniferous high-potassium I-type granitoid magmatism in the Eastern Pontides: The Gümüşhane pluton (NE Turkey). *Lithos* 2010, *116*, 92–110.

[61] Kaygusuz, A., Aydınçakır, E., Yücel, C., Atay, H.E., Petrographic and geochemical characteristics of carboniferous plutonic rocks around Erenkaya (Gümüşhane, NE Turkey). *J. Eng. Res. Appl. Sci.* 2021, *10*, 1774–1788.

[62] Vural, A., Kaygusuz, A., Petrology of the Paleozoic Plutons in Eastern Pontides: Artabel Pluton (Gümüşhane, NE Turkey). *J. Eng. Res. Appl. Sci.* 2019, *8*, 1216–1228.

[63] Kaygusuz, A., Geochronological age relationships of Carboniferous Plutons in the Eastern Pontides (NE Turkey). *J. Eng. Res. Appl. Sci.* 2020, *9*, 1299–1307.

[64] Karslı, O., Dokuz, A., Kandemir, R., Subduction-related Late Carboniferous to Early Permian Magmatism in the Eastern Pontides, the Camlik and Casurluk plutons: Insights from geochemistry, whole-rock Sr–Nd and in situ zircon Lu–Hf isotopes, and U–Pb geochronology. *Lithos* 2016, *266–267*, 98–114.

[65] Kaygusuz, A., Arslan, M., Siebel, W., Sipahi, F., et al., Geochronological evidence and tectonic significance of Carboniferous magmatism in the southwest Trabzon area, eastern Pontides, Turkey. *Int. Geol. Rev.* 2012, *54*, 1776–1800.

[66] Kaygusuz, A., Arslan, M., Sipahi, F., Temizel, İ., U-Pb zircon chronology and petrogenesis of Carboniferous plutons in the northern part of the Eastern Pontides, NE Turkey: Constraints for Paleozoic magmatism and geodynamic evolution. *Gondwana Res.* 2016, *39*, 327–346.

[67] Çoğulu, E., Gümüşhane ve Rize granitik plutonlarının mukayeseli petrojeolojik ve jeokronolojik etüdü. *Unpubl. Diss. Thesis, İstanbul Tech. Univ.* 1975.

[68] Yılmaz, Y., Petrology and structure of the Gümüşhane Granite and surrounding rocks, North-Eastern Anatolia. *PhD Thesis, Univ. London* 1972, 260 p.

[69] Saydam Eker, Ç., Petrography and geochemistry of Eocene sandstones from eastern Pontides (NE TURKEY): Implications for source area weathering, provenance and tectonic setting. *Geochemistry Int.* 2012, *50*, 683–701.

[70] Ağar, Ü., Geology of Demirözü (Bayburt) and Köse (Kelkit), KTU, Trabzon, 1977.

[71] Ustaömer, T., Robertson, A.H.F., Ustaömer, P.A., Gerdes, A., et al., Constraints on variscan and cimmerian magmatism and metamorphism in the pontides (Yusufeli-Artvin area), NE Turkey from U-Pb dating and granite geochemistry. *Geol. Soc. Spec. Publ.* 2013, *372*, 49–74.

[72] Pelin, S., Alucra (Giresun) Güneydoğu yöresinin petrol olanaklan bakımından jeolojik incelemesi, Karadeniz Teknik Üniversitesi Yayını, Yayın No. 87, Trabzon 1977.

[73] Sipahi, F., Vural, A., Akpinar, I., Saydam Eker, Ç., et al., Comparison of Fluid Inclusions of Egrikar Fe-Cu, Kopuz Fe And Karadag Fe-Cu Skarns Occurrences (Gümüshane, Turkey), in: *3rd International Conference on Engineering and Natural Science I(CENS 2017)*, 2017, pp. 561–561.

[74] Temizel, İ., Arslan, M., Yücel, C., Abdioğlu Yazar, E., et al., U-Pb geochronology, bulk-rock geochemistry and petrology of Late Cretaceous syenitic plutons in the Gölköy (Ordu) area (NE Turkey): Implications for magma generation in a continental arc extension triggered by slab roll-back. *J. Asian Earth Sci.* 2019, *171*, 305–320.

[75] Köprübaşı, N., Şen, C., Kaygusuz, A., Doğu Pontid adayayı granitoyidlerinin karşılaştırılmalı petrografik ve kimyasal özellikleri, KD Türkiye. *Uygulamalı Yerbilim. Derg.* 2000, *1*, 111–120.

[76] Kaygusuz, A., Saydam Eker, Ç., Geochemical features and petrogenesis of Late Cretaceous subduction-related volcanic rocks in the Değirmentaşı (Torul/Gümüşhane) area, Eastern Pontides (NE Turkey). *J. Eng. Res. Appl. Sci.* 2021, *10*, 1689–1702.

[77] Kaygusuz, A., Arslan, M., Temizel, İ., Yücel, C., et al., U–Pb zircon ages and petrogenesis of the Late Cretaceous I-type granitoids in arc setting, Eastern Pontides, NE Turkey. *J. African Earth Sci.* 2021, *174*, 104040.

[78] Kaygusuz, A., Siebel, W., Şen, C., Satir, M., Petrochemistry and petrology of I-type granitoids in an arc setting: The composite Torul pluton, Eastern Pontides, NE Turkey. *Int. J. Earth Sci.* 2008, *97*, 739–764.

[79] Tokel, S., Doğu Karadeniz bölgesinde Eosen yaşlı kalkalkalen andezitler ve jeotektonizma. *Türkiye Jeol. Kurult. Büllteni* 1977, *20*, 49–54.

[80] Karslı, O., Chen, B., Aydın, F., Şen, C., Geochemical and Sr-Nd-Pb isotopic compositions of the Eocene Dölek and Sariçiçek Plutons, Eastern Turkey: Implications for magma interaction in the genesis of high-K calc-alkaline granitoids in a post-collision extensional setting. *Lithos* 2007, *98*, 67–96.

[81] Topuz, G., Okay, A.İ., Altherr, R., Schwarz, W.H., et al., Post-collisional adakite-like magmatism in the Agvanis Massif and implications for the evolution of the Eocene magmatism in the Eastern Pontides (NE Turkey). *Lithos* 2011, *125*, 131–150.

[82] Kaygusuz, A., Sipahi, F., Ilbeyli, N., Arslan, M., et al., Petrogenesis of the late Cretaceous Turnagöl intrusion in the eastern Pontides: Implications for magma genesis in the arc setting. *Geosci. Front.* 2013, *4*, 423–438.

[83] Aslan, Z., Arslan, M., Temizel, İ., Kaygusuz, A., K-Ar dating, whole-rock and Sr-Nd isotope geochemistry of calc-alkaline volcanic rocks around the Gümüşhane area: Implications for post-collisional volcanism in the Eastern Pontides, Northeast Turkey. *Mineral. Petrol.* 2014, *108*, 245–267.

[84] Kaygusuz, A., Yücel, C., Arslan, M., Sipahi, F., et al., Petrography, mineral chemistry and crystallization conditions of Cenozoic plutonic rocks located to the north of Bayburt (Eastern Pontides, Turkey). *Bull. Miner. Res. Explor.* 2018, *157*, 75–102.

[85] Kaygusuz, A., Merdan Tutar, Z., Yücel, C., Mineral chemistry, crystallization conditions and petrography of Cenozoic volcanic rocks in the Bahçecik (Torul/Gumushane) area, Eastern Pontides (NE Turkey). *J. Eng. Res. Appl. Sci.* 2017, *6*, 641–651.

[86] Kaygusuz, A., Gucer, M.A., Yücel, C., Aydınçakır, E., et al., Petrography and crystallization conditions of Middle Eocene volcanic rocks in the Aydıntepe-Yazyurdu (Bayburt) area, Eastern Pontides (NE Turkey). *J. Eng. Res. Appl. Sci.* 2019, *8*, 1205–1215.

[87] Temizel, İ., Arslan, M., Ruffet, G., Peucat, J.J., Petrochemistry, geochronology and Sr–Nd isotopic systematics of the Tertiary collisional and post-collisional volcanic rocks from the Ulubey (Ordu) area, eastern Pontide, NE Turkey: Implications for extension-related origin and mantle source characteristi. *Lithos* 2012, *128–131*, 126–147.

[88] Temizel, İ., Arslan, M., Yücel, C., Abdioğlu Yazar, E., et al., Eocene tonalite–granodiorite from the Havza (Samsun) area, northern Turkey: adakite-like melts of lithospheric mantle and crust generated in a post-collisional setting. *Int. Geol. Rev.* 2020.

[89] Yücel, C., Arslan, M., Temizel, İ., Abdioğlu Yazar, E., et al., Evolution of K-rich magmas derived from a net veined lithospheric mantle in an ongoing extensional setting: Geochronology and geochemistry of Eocene and Miocene volcanic rocks from Eastern Pontides (Turkey). *Gondwana Res.* 2017, *45*, 65–86.

[90] Kaygusuz, A., Şahin, K., Mescitli (Torul / Gümüşhane) ve Çevresindeki Eosen Yaşlı Volkanik Kayaçların Petrografik, Jeokimyasal ve Petrolojik Özellikleri. *Gümüşhane Üniversitesi Fen Bilim. Enstitüsü Derg.* 2016, *6*, 89.

[91] Kaygusuz, A., Aslan, Z., Aydınçakır, E., Yücel, C., et al., Geochemical and Sr-Nd-Pb isotope characteristics of the Miocene to Pliocene volcanic rocks from the Kandilli (Erzurum) area, Eastern Anatolia (Turkey): Implications for magma evolution in extension-related origin. *Lithos* 2018, *296–299*, 332–351.

[92] Vural, A., Kaygusuz, A., Geochronology, petrogenesis and tectonic importance of Eocene I-type magmatism in the Eastern Pontides, NE Turkey. *Arab. J. Geosci.* 2021, *14*, 467.

[93] Aydınçakır, E., Yücel, C., Ruffet, G., Gücer, M.A., et al., Petrogenesis of post-collisional Middle Eocene volcanism in the Eastern Pontides (NE, Turkey): Insights from geochemistry, whole-rock Sr-Nd-Pb isotopes, zircon U-Pb and 40Ar-39Ar geochronology. *Geochemistry* 2022, 125871.

[94] Kaygusuz, A., K/Ar ages and geochemistry of the post-collisional volcanic rocks in the Ilica (Erzurum) area, eastern Turkey. *Neues Jahrb. Fur Mineral.* 2009, *186*, 21–36.

[95] Vural, A., Külekçi, G., Zenginleştirilmiş Jeoturizm Güzergahı:Gümüşhane-Bahçecik Köyü. *Euroasia J. Math. Eng. Nat. Med. Sci.* 2021, *8*, 1–23.

[96] Vural, A., Zenginleştirilmiş Jeoturizm Güzergahlarına Dair Farkındalık Olusturulması: Eski Gümüshane-Dört Konak Güzergahı, in: *II. International Sustainable Tourism Congress*, Gümüşhane, Türkiye 2018, pp. 533–542.

[97] Vural, A., Gümüshane-Zigana Zenginleştirilmiş Jeoturizm Güzergâhı, in: *II. International Sustainable Tourism Congress*, Gümüşhane, Türkiye 2018, pp. 607–617.

[98] Vural, A., Zenginleştirilmiş Jeoturizm Güzergahlarına Dair Farkındalık Oluşturulması : Eski Gümüşhane - Dörtkonak Güzergahı. *Gümüşhane Üniversitesi Sos. Bilim. Enstitüsü Elektron. Derg.* 2019, *10*, 250–274.

[99] Vural, A., Külekçi, G., Bahçecik (Gümüşhane) ve Yakın Civarı Zenginleştirilmiş Jeoturizm Güzergahı, in: *UMTEB 11.Uluslararası Mesleki ve Teknik Bilimler Kongresi*, Ankara, Türkiye 2021.

[100] Güven, İ.H., Doğu Pontidlerin 1/100.000 Ölçekli Kompilasyonu, MTA Genel Müdürlüğü, Ankara 1993.

[101] Vural, A., Kaygusuz, A., Avliyana (Torul-Gümüşhane) Antimonit Cevherleşmesinin Jeolojisi-Mineralojisi ve Kökeninin Araştırılması, Gümüşhane, Türkiye 2016.

[102] Vural, A., Kaygusuz, A., Dönmez, H., Avliyana Antimonit Cevherleşmesinin Duraylı İzotop ve Sıvı Kapanım Verileriyle Değerlendirilmesi, in: *69. Türkiye Jeoloji Kurultayı*, Ankara, Türkiye 2016, pp. 370–373.

[103] Vural, A., Kaygusuz, A., Paleozoyik Yaşlı Artabel Plütonunun (Gümüşhane) Petrografik ve Jeokimyasal Özellikleri, in: *3. Uluslararası GAP Matematik-Mühendislik-Fen ve Sağılık Bilimleri Kongresi*, İKSAD, Şanlıurfa, Türkiye 2019.

[104] Vural, A., Zenginleştirilmiş Jeoturizm Rotası: Karadağ ve Artabel Gölleri, in: *71. Türkiye Jeoloji Kurultayı*, Ankara, Türkiye 2018, pp. 481–482.

[105] Güner, S., Yazıcı, E.N., Dursun, A., Yılmaz, Z., et al., Gümüşhane-Bayburt-Trabzon Polimetal Ruhsat Sahaları Jeoloji Raporu, Ankara, Türkiye 2003.

[106] Eren, M., Gümüşhane-Kale Arasının Jeolojisi ve Mikrofasiyes incelemesi, Karadeniz Teknik Üniversitesi, 1983.

[107] Vural, A., Kaygusuz, A., Kirlilik Parametrelerine Göre Farklı Kayaçların Element İçeriklerinin Araştırılması: Avliyana (Torul-Gümüşhane/Türkiye), in: *2. Uluslararası Hasankeyf Bilimsel Araştırmalar ve İnovasyon Kongresi*, Batman, Türkiye 2022, pp. 251–259.

[108] Vural, A., Canca (Gümüşhane) Alterasyon Sahasında Toprak ve Bitki Jeokimyası Çalışmaları ile Altın Potansiyelinin Araştırılması, Ankara, Türkiye 2014.

[109] Vural, A., Toprak ve Akasya ağacı sürgünlerindeki iz/ağır metal dağılımı, Gümüşhane-Türkiye. *MTA Derg.* 2014, *148*, 85–106.

[110] Vural, A., Gundogdu, A., Akpinar, I., Baltaci, C., Environmental impact of Gümüşhane City, Turkey, waste area in terms of heavy metal pollution. *Nat. Hazards* 2017, *88*, 867–890.

[111] Vural, A., Erdoğan, M., Eski Gümüşhane Kırkpavli Alterasyon Sahasında Toprak Jeokimyası. *Gümüşhane Üniversitesi Fen Bilim. Enstitüsü Derg.* 2014, *4*, 1–15.

[112] Bulut, V.N., Gundogdu, A., Duran, C., Senturk, H.B., et al., A multi-element solid-phase extraction method for trace metals determination in environmental samples on Amberlite XAD-2000. *J. Hazard. Mater.* 2007, *146*, 155–163.

[113] Muller, G., Index of geoaccumulation in sediments of the Rhine River. *Geol. J.* 1969, *2*, 108–118.

[114] Rudnick, R., Gao, S., Composition of the Continental Crust, in: Holland, H., Turekian, K. (Eds.), *Readings of Treatise on Geochemistry*, 2nd ed., Elsevier, Londan, England 2010, pp. 101–123.

[115] Stoffers, P., Glasby, G.P., Wilson, C.J., Davis, K.R., et al., Heavy metal pollution in Wellington Harbour. *New Zeal. J. Mar. Freshw. Res.* 1986, *20*, 495–512.

[116] Sutherland, R.A., Bed sediment-associated trace metals in an urban stream, Oahu, Hawaii. *Environ. Geol.* 2000, *39*, 611–627.

[117] Tomlinson, D.L., Wilson, J.G., Harris, C.R., Jeffrey, D.W., Problems in the assessment of heavy-metal levels in estuaries and the formation of a pollution index, 1980.